

High temperature structural studies in palygorskite

P. S. MUKHERJEE

Regional Research Laboratory (CSIR), Trivandrum 695 019, India

S. LOKANATHA, S. BHATTACHERJEE

Indian Institute of Technology, Kharagpur 721 302, India

The dehydration transformation in a palygorskite sample has been studied by XRD, by applying the three-phase model consisting of crystalline, non-crystalline and paracrystalline domains. Measurements of the structural parameters characterizing the three domains, showed that crystallinity of the sample increased whereas distortion decreased up to 300 °C at which temperature anhydride phase developed. At higher temperatures, distortion, non-crystallinity and paracrystallinity increased, resulting in the formation of an admixture of anhydride and amorphous phases due to the expulsion of the entire co-ordinate and some hydroxyl water. The variations of the structural disorder was found to be anisotropic. The (1 1 0) planes were more vulnerable to disorder than the (0 1 0) planes.

An attempt was also made to correlate the variations of the structural parameters with that of the dielectric properties. The variations of dielectric constant and dielectric loss were found to be related to the amorphous and paracrystalline domains.

1. Introduction

Palygorskite is a clay mineral with double silica chains (ribbons) with various types of structural disorder related to vacancies in the octahedral sites [1] and to ribbon displacements both parallel and perpendicular to the fibre axis [2, 3, 6]. This mineral contains four different types of water which have been described as hygroscopic, zeolitic, co-ordinated and hydroxyl water; each of which is lost at a different temperature range. The dehydration transformation has been explained [5, 6] on the basis of a folding mechanism of the chains, presuming the interchain bond forces to be weak as also observed in fibrous polymers [6–8]. Attempts have been made [2, 3] to explain this transformation in terms of two types of layer disorders and showed that the defect model is compatible with the concept of a folding mechanism. These structural disorders increase at higher temperatures as have been revealed by X-ray powder diffraction and infrared spectroscopic studies [2, 9]. Palygorskite and its high temperature transformation products may be considered to consist of three types of structural domains, crystalline, paracrystalline, and amorphous [7]. Usually such fibrous material is assumed to consist of crystalline and non-crystalline regions, however, the highly broadened diffraction profiles and the absence of higher order reflections in the X-ray powder pattern of the palygorskite sample, as observed by the present authors, indicate the existence of a third, poorly crystalline region [8] which was first termed paracrystalline [10]. "Paracrystallinity" represents an intermediate structural state between fully crystalline and non-crystalline states. In the paracrystalline state,

the periodicity of the chains or linear crystallites composing the material is more or less preserved, but their orientations are disordered. A three-state model consisting of crystalline, paracrystalline and non-crystalline domains may thus represent better the structural states of palygorskite and its dehydration products. An attempt has, therefore, been made in the present work to study the dehydration transformation in palygorskite in terms of this three-domain model.

2. Theory

The three-domain model [7] envisages the coexistence of crystalline, paracrystalline and non-crystalline domains distributed randomly in the entire body of the sample without any sharp boundaries. According to these authors, the total intensity $I(s)$, of X-rays scattered in the direction s from a system composed of the three domains is given by

$$I(s) = I_c + I_p + I_{nc}$$

where I_c , I_p , and I_{nc} are the scattered intensities from the crystalline, paracrystalline and non-crystalline domains, respectively. The three most important parameters characterizing a three-domain model are degree of crystallinity (X_c), degree of paracrystallinity (X_p) and degree of non-crystallinity (X_{nc}) and are defined as $X_c = I_c/I$, $X_p = I_p/I$, and $X_{nc} = I_{nc}/I$, respectively. Each of these parameters represents the proportion of the corresponding phase in the entire sample. The paracrystalline phase is further characterized by two additional texture parameters, namely domain size (M) and distortion (D). Distortion is

defined as the mean deviation in the position of atoms in the paracrystalline state from the structural site in the corresponding crystalline state. This set of parameters characterizing a substance having three domains will be, hereinafter, referred to as structural parameters. The experimental evaluation of these parameters is based on the variance (W) and the integral width (β) of the resultant diffraction profile of I_p and I_c which were defined [7] as

$$W = \frac{\sigma}{2\pi^2} \left(\frac{1}{M} + P_2 D \right) - \frac{1}{4\pi^2} P_2 D \left(\frac{2}{M} + D \right)$$

and

$$\beta = \frac{1}{P_1 M + P_2 / (D + 1/M)}$$

where P_1 and P_2 are fractions of diffracted intensities from the crystalline and non-crystalline components, respectively, and σ is the range of the diffraction profile for estimating W and β . From the slope and intercept of the linear plot of W against σ and the integral width, all the structural parameters can be calculated.

3. Experimental procedure

The present investigation was carried out on a specimen of palygorskite from Florida (PF1-1, from the Source Clay Repository of The Clay Minerals Society). Details of the sample preparation and results of chemical and differential thermal analyses were already reported [2].

The XRD patterns were recorded on a Philips Norelco diffractometer using $\text{CuK}\alpha$ radiation at 35 kV and 10 mA and a Ni-Al balanced filter. The 110 and 040 reflections, found suitable for analysis, were

recorded at intervals of 0.05° (2θ) applying fixed-step scanning method. Annealed quartz powder of large crystallite size was used to obtain the pattern for instrumental corrections. Necessary corrections for background and various physical factors affecting the observed intensities were made [7, 8]. The variance-range curves were obtained using a 1030 computer. Dielectric measurements of the hot-pressed samples were carried out following standard procedure [11].

4. Results and discussions

Figs 1 and 2 show the XRD intensity distribution of palygorskite samples heated to different temperatures. Figs 3 and 4 depict the corrected 110 reflections of the samples at different temperatures and their corresponding variance-range plots, respectively. Similar variance-range curves (not shown) were also drawn for 040 reflection. The slopes and intercepts of the variance-range curves of the 110 and 040 reflections are shown in Table I. The different structural parameters of the three-domain model as described above, were calculated [12] and are listed in Table II. The observed temperature variations of the dielectric constant and dielectric loss of the sample are shown in Figs 5 and 6, respectively.

As shown by the data in Table II, the degree of crystallinity (X_c) and domain size (M) increased and the degree of non-crystallinity (X_{nc}) gradually decreased to 300°C . The variations do not, however, follow any regular pattern. Above 300°C , the non-crystalline fraction (X_{nc}) increased appreciably and the crystalline fraction decreased markedly. These variations are accompanied by an appreciable rise in the distortion (D) and a reduction in the paracrystallite size. This trend continued to 800°C at which

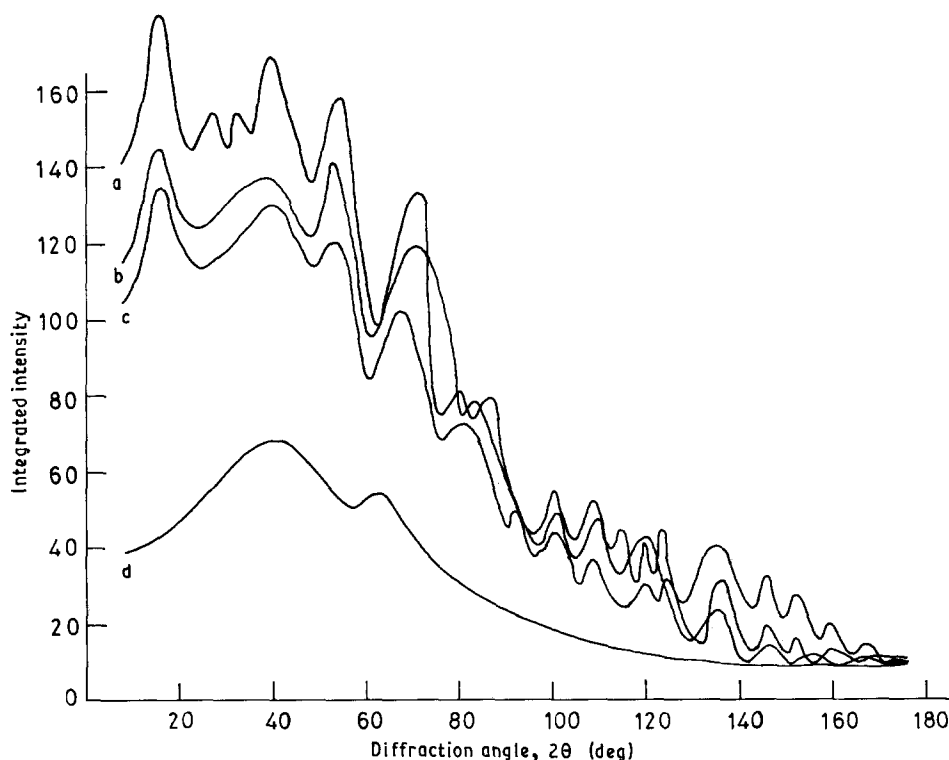


Figure 1 Scattered intensity distribution of palygorskite at (a) 300°C , (b) 200°C , (c) 28°C and (d) amorphous and of non-crystalline state.

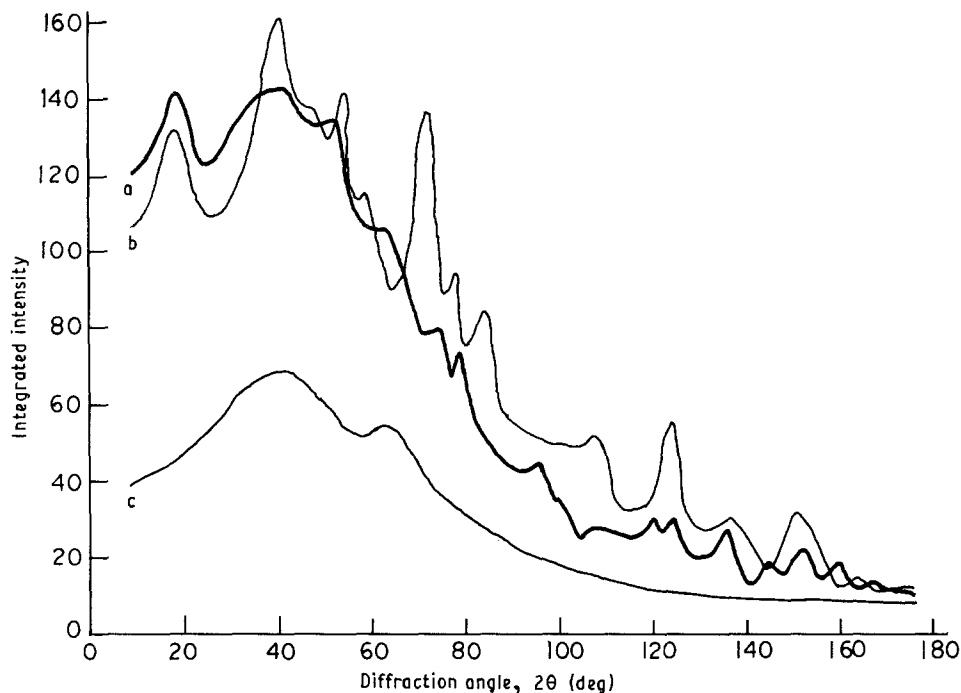


Figure 2 Scattered intensity distribution of palygorskite at (a) 500 °C (b) 400 °C and (c) amorphous and of non-crystalline state.

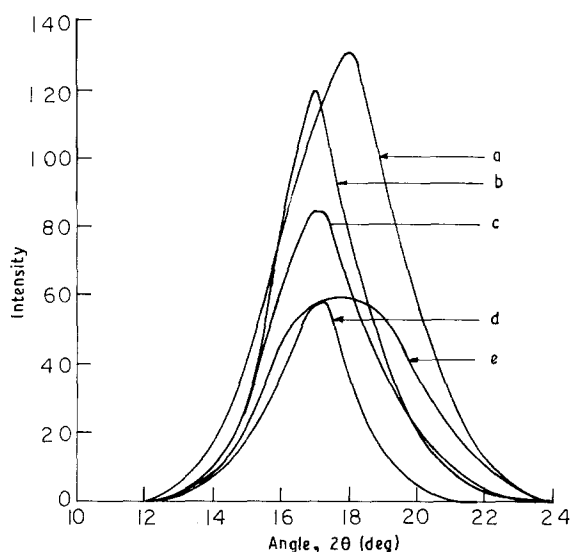


Figure 3 Intensity distribution of 110 reflection of palygorskite at different temperatures (a 300 °C, b 200 °C, c 28 °C, d 400 °C, e 500 °C).

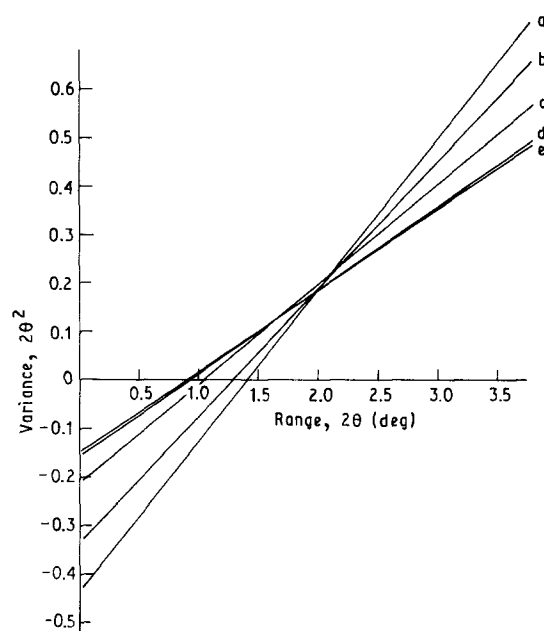


Figure 4 Variance-range curves for the 110 reflection of palygorskite at different temperatures (a 500 °C, b 400 °C, c 28 °C, d 200 °C, e 300 °C).

temperature the ordered structure was found to be destroyed. The diffraction pattern at this temperature consisted of a broad diffuse halo characteristic of non-crystalline material.

The structural parameters as derived from the 110 and 040 reflections also varied anisotropically. It is also seen from Table II, that the values of X_c corresponding to both these reflections increased whereas values of D decreased up to 300 °C. X_c increased more and D also decreased less markedly than in (010) direction at all temperatures below 300 °C [10]. These observations suggest that the atomic arrangement in and stacking of the (110) planes were more ordered than those of the (010) planes. This observation is consistent with the results of electron microscope and

XRD studies [2, 13] which clearly demonstrate that the (100) and (110) planes form the cleavage faces of the palygorskite laths parallel to the fibre axis as in sepiolite [1]. The lattice structure, however, remained more or less intact up to 300 °C above which X_c started decreasing and D increasing, steadily. This trend suggests that the degree of disorder increased, marking the onset of the structural breakdown above 300 °C. The variations of X_c and D along the (110) and (010) directions indicate that (110) planes are more vulnerable to structural disorder than (010) planes. This behaviour may be attributed to folding of

TABLE I Results of various range analysis of the X-ray powder diffraction profiles of 110 and 040 reflections at different temperatures

Temperature (°C)	110 reflection		040 reflection	
	Slope $\times 10^{-2}$ <i>I</i> (nm)	Intercept $\times 10^{-2}$ <i>I</i> (nm)	Slope $\times 10^{-2}$ <i>I</i> (nm)	Intercept $\times 10^{-4}$ <i>I</i> (nm)
28 ^a	0.441	1.052	0.752	2.541
200	0.376	0.776	0.659	2.085
300	0.366	0.752	0.468	1.075
400	0.538	1.654	0.501	1.367
500	0.668	2.159	0.703	2.300

^a Room temperature.

TABLE II Structural parameters of palygorskite at different temperatures

Structural parameters	Temperature									
	28°C		200°C		300°C		400°C		500°C	
	110	040	110	040	110	040	110	040	110	040
Degree of crystallinity, X_c (%)	22	17	30	24	32	26	18	18	14	14
Degree of paracrystallinity, X_p (%)	33	38	29	35	32	38	41	41	40	40
Degree of non-crystallinity, X_{nc} (%)	45	45	41	41	36	36	41	41	40	40
Paracrystallite size, M (nm)	3.2	1.9	3.6	2.0	3.8	2.9	2.7	2.8	2.0	1.9
Distortion, D (%)	1.25	1.90	1.10	1.60	1.00	1.20	1.70	1.50	1.80	1.80

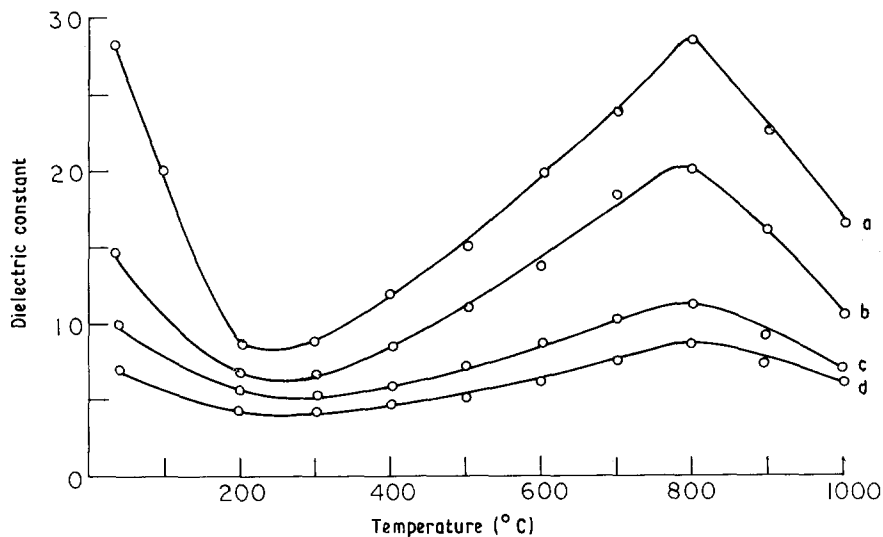


Figure 5 Variation of dielectric constant (K) with temperature at different frequencies (a 5×10^2 Hz, b 10^4 Hz, c 10^5 Hz, d 10^6 Hz).

the double chains around the lines of oxygen atoms that was caused by the expulsion of the coordinated water and which resulted in more distortion along (110) than (010). This anisotropy can also be ascribed to critical anisotropic thermal vibrations of the molecules above 300°C. Another explanation may be that the expulsion of the water molecules from the microchannels introduced variability of interlayer spacings of the cleavage plane (110), which increased with temperature [2, 13].

The different phases representing the various dehydration stages of the sample can be identified with the different structural states [13] and studied in terms

of particle size [14]. The crystalline phase at 200°C corresponded to the state when all the zeolitic water along with some coordinated water escaped resulting in an increase of X_c as shown in Table II and in particle size along (110) and (010). The phase with highest degree of crystallinity that developed at 300°C may be identified with the anhydride state when most of the coordinated water escaped with the appearance of a new line at 0.92 nm and setting in the ordered folded state as was also observed earlier [5]. The high temperature phases at 400 and 500°C with poor crystallinity (X_c) and high order of distortion (D) represented the structural state which consisted of an

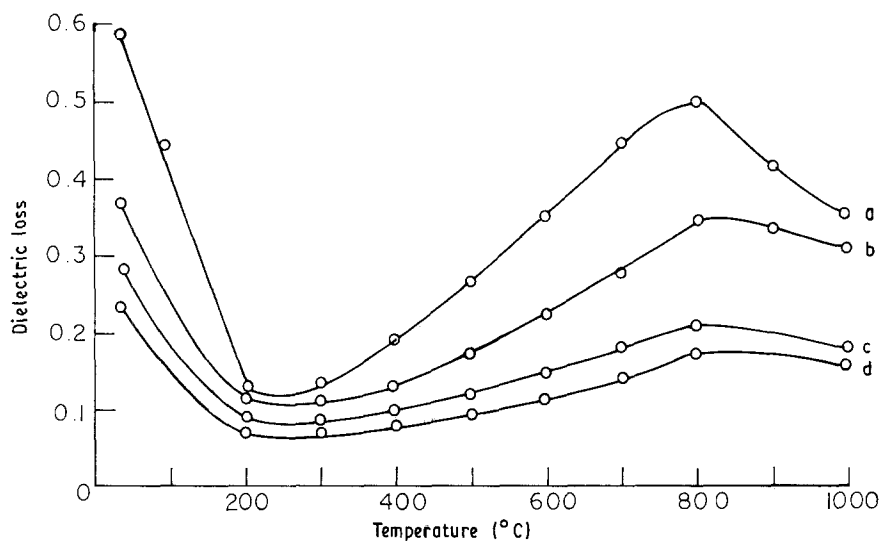


Figure 6 Variation of dielectric loss ($\tan \delta$) with temperature at different frequencies (a 5×10^2 Hz, b 10^4 Hz, c 10^5 Hz, d 10^6 Hz).

admixture of anhydrous and amorphous forms resulting from the expulsion of the admixture co-ordinated water and partial removal of (OH) water. At 500°C, more hydroxyl water escaped. Consequently the structure collapsed more resulting in further decrease of X_c and increase of D as shown in Table II. X_{nc} and X_p , however, remained more or less the same.

An attempt is also made to correlate the dielectric and structural properties of this mineral at different temperatures, similar to those reported for disordered polymers [6]. It has been reported that the degree of non-crystallinity was mainly responsible for high dielectric constant and dielectric loss in a poorly crystalline material whereas the paracrystalline region with considerable distortion constituted the next most important factor. According to this observation and the structural parameters listed in Table II, both dielectric constant and dielectric loss should increase up to 300°C. Above 300°C these parameters should again increase with an increase of X_{nc} and D . As expected the experimentally measured values of these dielectric parameters follow exactly the same type of temperature variation as mentioned (Figs 5 and 6).

Acknowledgement

The authors thank G. B. Mitra for his encouragement and K. V. Rao for his help in taking the dielectric measurements.

References

1. G. W. BRINDLEY, "Crystal Structure of Clay Minerals and their X-ray Identification" (Mineralogical Society, London, 1980) 125.
2. S. LOKANATHA and S. BHATTACHERJEE, *Clay Mineral.* **19** (1984) 253.
3. *Idem.*, *Ind. J. Pure Appl. Phys.* **22** (1984) 719.
4. C. SERNA, J. L. AHLEIXKA and J. M. SERRATOSA, *Clays & Clay Minerals* **23** (1975) 452.
5. G. E. Van SCOYOC, C. SERNA and J. L. AHIRICHS, *Amer. Mineral.* **69** (1979) 215.
6. P. S. MUKHERJEE, PhD thesis, Indian Institute of Technology, Kharagpur, India (1981).
7. G. B. MITRA and P. S. MUKHERJEE, *Polymer* **21** (1980) 1403-1409.
8. *Idem.*, *J. Appl. Crystallogr.* **14** (1981) 421.
9. H. HAYASHI, R. OTSUKA and N. IMANI, *Amer. Mineral.* **54** (1969) 1613.
10. R. HOSEMANN and S. N. BAGCHI, "Direct Analysis of Diffraction by Matter" (Elsevier, Amsterdam, 1962).
11. S. LOKANATHA and S. BHATTACHERJEE, *J. Mater. Sci. Lett.* **3** (1984) 299.
12. P. S. MUKHERJEE and G. B. MITRA, *Polymer* **24** (1983) 524.
13. S. BHATTACHERJEE and S. LOKANATHA, *Trans. Ind. Ceram. Soc.* **43** (1984) 149.
14. S. LOKANATHA and S. BHATTACHERJEE, *Ind. J. Pure Appl. Phys.* **23** (1985) 403.

Received 5 June 1990

and accepted 31 January 1991